Journal of Electrical Engineering and Renewable Energies Development (JEERED)
Issue N°: 1 , Vol. N°: 1, pp. 9-16, 2025

QFT Controller Of Switched Reluctance Motor

Ahmed TAHOUR [1], Abdel Ghani AISSAOUI [2]
(1) Ecole supérieure en sciences techniques ESSA Tlemcen 13000 Alegria
(2) University Tahri Mohamed of Bechar, 08000, Algeria

***Abstract*—** This study presents the implementation of Quantitative Feedback Theory (QFT) for the robust speed control of a variable reluctance motor (SRM). Introduced by Isaac Horowitz, QFT is a robust control approach formulated in the frequency domain, allowing for the systematic handling of parametric uncertainties and external disturbances while respecting predefined performance constraints. Unlike classical control strategies, which are generally based on a nominal model of the system, QFT explicitly considers a set of uncertainties describing the possible variations of the model. This consideration guarantees both robust stability and performance maintenance throughout the uncertainty range. Applied to SRM control, the proposed method significantly improves the dynamic response, disturbance rejection capability, and system stability margins. Simulation results and experimental tests confirm that the QFT controller provides more precise speed regulation, faster transient response and increased robustness to parametric variations and load disturbances, compared to conventional proportional-integral (PI) control.

Keywords—S*witched reluctance motor, PI, Quantitative Feedback Theory (QFT), Speed control.*

I. INTRODUCTION

Switched reluctance motors (SRMs) are distinguished by their robust construction and significant economic advantages, making them particularly well-suited to a wide range of industrial applications. Their structural simplicity results from a salient-pole stator with concentrated windings, allowing for shorter turns and easier manufacturing, and a salient-pole rotor devoid of conductors and permanent magnets, representing the simplest rotor architecture available.

This robust and streamlined design gives SRMs low production costs, increased reliability, and, when combined with high-speed operation and a high torque-to-inertia ratio, makes them a preferred candidate for industrial applications requiring high dynamic performance and long service life [1].

Model uncertainty significantly complicates controller design, as the controller must meet performance specifications not only for a nominal model with fixed parameters, but also for all possible models within the uncertainty range. Independent analysis or synthesis of an optimal controller for each system configuration—in other words, a brute-force approach—proves extremely time-consuming, if not practically impractical [2].

Robust control engineering is thus a branch of control engineering dedicated to explicitly addressing modeling uncertainties and designing reliable control laws capable of ensuring the required stability and performance across all real-world system models..

Quantitative Feedback Theory (QFT), introduced by Isaac Horowitz, is a robust control method formulated in the frequency domain, specifically designed for systems subject to parametric uncertainties and significant disturbances. Its fundamental principle is based on the explicit consideration of the trade-off between performance, robustness, and controller complexity.

Unlike classical approaches based on a single nominal model, QFT allows the synthesis of a single, invariant controller capable of guaranteeing the desired performance for all possible models of the system. This property is obtained by translating the performance specifications and model uncertainties into design boundaries on the Nichols diagram, which serves as a graphical representation of the loop shaping process [2].

Quantitative Feedback Theory (QFT) is an innovative design methodology for developing robust controllers capable of maintaining desired performance despite system uncertainties. Its main strength lies in the quantitative determination of the feedback level required to meet performance specifications in an uncertain environment.

QFT relies on the use of frequency bounds to guide a manual loop shaping process, thus providing the designer with a deep understanding of the trade-offs between robustness, performance, and complexity. While this approach requires advanced expertise in frequency analysis and control synthesis, it enables the development of transparent controllers with rigorously guaranteed performance and stability.

This paper details the application of Quantitative Feedback Theory (QFT) for speed control of a switched reluctance motor (SRM). It is organized as follows: Section II outlines the control principles of an SRM drive. Section III and IV introduce the proposed QFT controller and its application to SRM speed regulation, supported by simulation results demonstrating its effectiveness. Finally, Section V presents the concluding remarks.

II. SRM MODEL

A. *Description of the system*

The switched reluctance machine (SRM) is distinguished by its particularly simple architecture, in which only the stator has windings, while the rotor, made entirely of rolled steel sheets, contains neither conductors nor permanent magnets. This robust and streamlined design contributes to a significant reduction in manufacturing costs and increased reliability. Thanks to this mechanical simplicity and recent advances in power electronics, the SRM has attracted increasing interest over the past decade, resulting in numerous studies and industrial applications. Compared to alternating current (AC) and direct current (DC) machines, the SRM offers two major advantages [3]:

• High reliability — each phase operates largely independently, both magnetically and electrically, which improves fault tolerance and simplifies maintenance.

• Very high speed operating capability — the absence of conductors and magnets in the rotor allows high rotational speeds, generally between 20,000 and 50,000 rpm, to be achieved while maintaining excellent mechanical and thermal stability.

Motion in an SRM is produced by the variable reluctance in the air gap. When a stator phase is energized, it creates a magnetic field, and reluctance torque is generated as the rotor moves to align with the position of minimum magnetic reluctance [4]. Figure (1) shows a cross-sectional view of the machine.

The schematic of the proposed speed control system is illustrated in Figure (2). The power circuit consists of an asymmetric H-bridge converter connected to the stator of the switched reluctance machine (SRM). Each phase of this converter comprises two IGBT transistors and two diodes connected in antiparallel, thus ensuring bidirectional switching of the phase current.

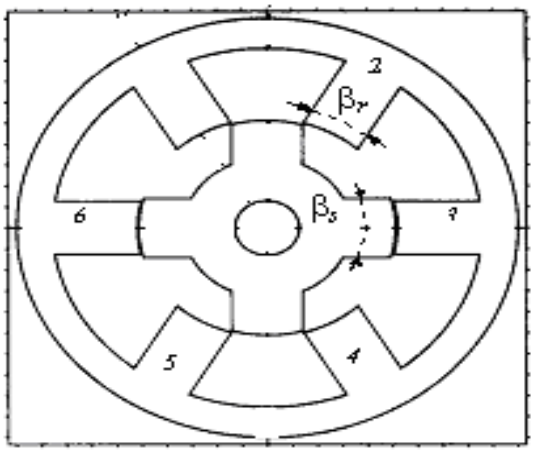

Fig. 1 – Switched reluctance motor

The QFT controller generates the control signal from the speed error, calculated as the difference between the speed reference and the measured value. This signal is then integrated to produce the current setpoint applied to the system. The characteristic parameters of the SRM used in this study are listed in the appendix [4, 5].

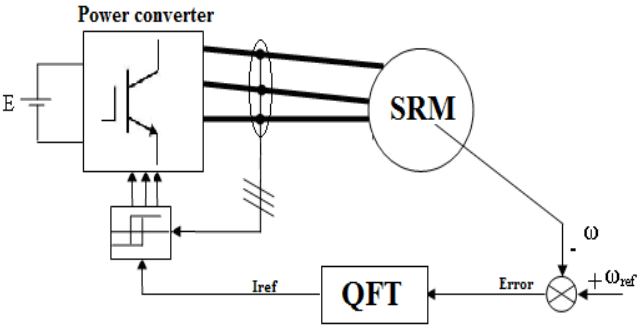

Fig. 2 – Control of SRM

B. *Machine equation*

Although SRM is mechanically simple, its mathematical modeling is challenging due to highly nonlinear behavior. This nonlinearity arises because the flux linkage is a function of two variables: the phase current (I) and the rotor position (θ). The model derived from the equivalent electrical circuit is given by:

$$V_j = RI_j + \frac{d\Psi_j(i,\theta)}{dt} \qquad (1)$$

Then we can write:

$$V_j = RI_j + \frac{d\Psi_j(i,\theta)}{di}\frac{di}{dt} + \frac{d\Psi_j(i,\theta)}{d\theta}\omega \qquad (2)$$

With $j = 1,.2.3$

where: $\omega = \frac{d\theta}{dt}$

The dynamic equation is:

$$J\frac{d\omega}{dt} = T_e - T_l - F\omega \tag{3}$$

The total average torque T_e is produced by the superposition of torque from each individual phase:

$$T_e = \sum_{phase=1}^{n} T_{phase} \tag{4}$$

where

$$T_{phase} = \frac{1}{2}\frac{dL(\theta,i)}{d\theta} i^2 \tag{5}$$

Where V : the terminal voltage, I : the phase current, R - the phase winding resistance, Ψ : the flux linked by the winding, J : the moment of inertia, F : the friction, $L(\theta,i)$: the instantaneous inductance and T_e is the total torque.

III. QUANTITATIVE FEEDBACK THEORY MODE SPEED CONTROLLER

A. *Quantitative Feedback Theory principle*

a) Step 1: Define Uncertainty & Generate Templates

Figure (3) illustrates the feedback structure adopted in the QFT design methodology. The plant P(s) is subject to parametric uncertainties and unknown disturbances D(s). The controller G(s) is designed to mitigate the impact of these uncertainties and disturbances on the plant output. In addition, it may incorporate a filtering function F(s) to shape the system response in accordance with the specified control requirements.

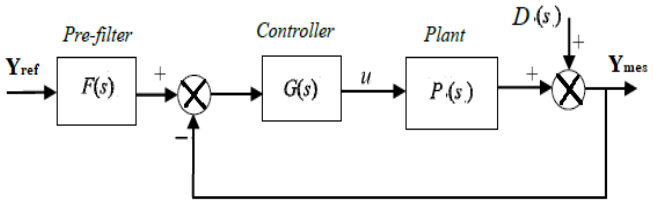

Fig. 3 –A closed-loop system.

b) Step 2: Specify Performance Requirements

QFT translates time-domain specs (e.g., overshoot, settling time) into frequency-domain bounds on the closed-loop transfer function. Common specs include:

- **Robust Stability:** Ensure all possible closed-loop systems are stable. Specified by a maximum peak of the closed-loop function

$$\left|H(jw)\right| = \left|\frac{Y_{mes}}{Y_{ref}}(jw)\right| = \left|\frac{P(jw).G(jw)}{1+P(jw).G(jw)}\right| \le M_t, \quad \forall w \in [0 \ \infty[\tag{6}$$

M_t which represent the locus of constant magnitude of the closed-loop transfer function in the Nichols chart

- **Reference Tracking:** Ensure the output Y(s) tracks the reference $Y_{ref}(s)$ within a tolerance band. Specified by upper and lower bounds

$$\left|m_l(jw)\right| \le \left|F(jw)\frac{P(j.w).G(j.w)}{1+P(j.w).G(j.w)}\right| \le \left|m_u(jw)\right|, \quad \forall w \in [0 \ \infty[\tag{7}$$

m_L and m_U are the system response time limit.

- **Disturbance Rejection:** Limit the output due to disturbances. Specified by a maximum magnitude

$$\left|S(jw)\right| = \left|\frac{Y_{mes}}{D}\right| = \left|\frac{1}{1+P(jw).G(jw)}\right| \le M_s, \quad \forall w \in [0 \ \infty[\tag{8}$$

M_s is the disturbance limit at the system output.

b) Step 3: Translate Specifications into Bounds

This is the heart of QFT. For each frequency ω and for each performance specification:

- Use the corresponding plant template { $P(jw)$ }.
- Calculate the maximum allowable closed-loop gain (from the specs).
- Mathematically translate this requirement into a constraint (bound) on the loop transfer function $L(jw) = P(jw).G(jw)$ on the Nichols Chart.
- This results ($L(jw)$) in a set of boundary curves for each frequency. The controller $G(jw)$ must be designed so that the nominal loop function $L_0(jw)$ lies on the correct side of *all* these bounds at their respective frequencies.

d) Step 4: Loop Shaping (Designing G(s))

The objective is to design a controller $G(jw)$ such that the Nominal Loop Function $L_0(jw) = P_0(jw).G(jw)$:

- Satisfies all bounds on the Nichols Chart at every frequency.
- Achieves this with the minimum possible gain **and** bandwidth (to avoid noise amplification, actuator saturation, and to ensure robustness).

$P_0(jw)$ is a specific plant chosen from the uncertain set $\{ P(jw) \}$, typically the "median" or "most representative" plant.

e) Step 5: Design the Pre-filter $F(s)$

The job of $F(s)$ is to fine-tune the reference tracking performance after $G(s)$ has been designed.

B. *Quantitative Feedback Theory controller*

Using equation (3) and using the Laplace transform, the mechanical equation is modeled as follows;

$$\frac{\omega(s)}{T_e(s)} = \frac{1}{J.s + F} \tag{9}$$

With $d = T_l$

Figure (4) presents the feedback control block diagram

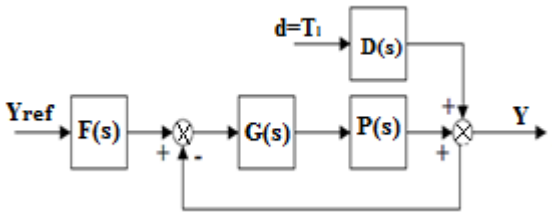

Fig. 4 –The feedback control block diagram

With two parameters with independent uncertainty Table 1.

TABLE I. PARAMETRIC UNCERTAINTY FOR SRM

Parameter	Unit	Percentage of variation
J	Kg/m^2	$13*10^{-4}$±50%
F	Nm/s	$183*10^{-4}$±50%

The frequency spectrum for this analysis ranges from 1 rad/s to 10,000 rad/s. To accurately capture the system's dynamics, particularly the slopes in the frequency response, this base range was augmented with additional points. The final frequency array, which is also provided in the QFT toolbox, is [6-16]:

w=[1 5 10 100 200 300 500 700 1000 2000 10000]rad/s

Figure (5) shows the bode plot of the plant.

Figure (6) illustrates the template generation process. On the Nichols chart, a template represents the set of possible frequency responses of the plant, considering all parametric uncertainties, at a specific frequency.

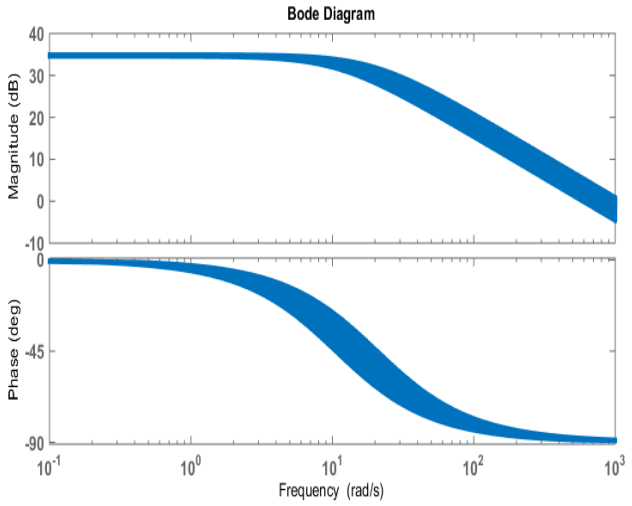

Fig. 5 – The bode plot of plants.

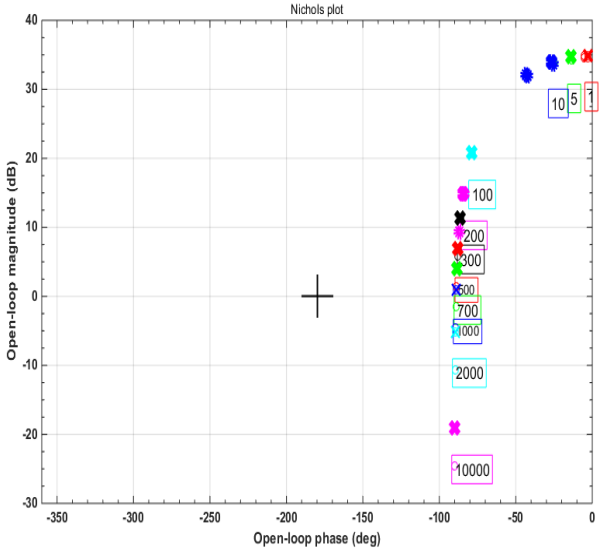

Fig. 6 –. The Nichols chart of plants of power plants.

C. *Performance Specifications*

a) Sensitivity or disturbances at plant output specification

While the disturbance rejection performance specifications are [6-12]::

$$\left| \frac{1}{1 + P(jw).G(jw)} \right| \le \frac{s / a_d}{s / a_d + 1} \tag{10}$$

with $a_d = 1000$

w=[1 5 10 20 40 60 80 100 200 300 500 700 1000] rad/s

b) Reference tracking specification:

Figures (7) shows the step responses for the upper, $m_u(\omega)$ and lower, $m_l(\omega)$, boundaries. Figure (7.a) presents the time-

domain responses, while Figure (7.b) shows their corresponding frequency-domain translations [6-16]:.

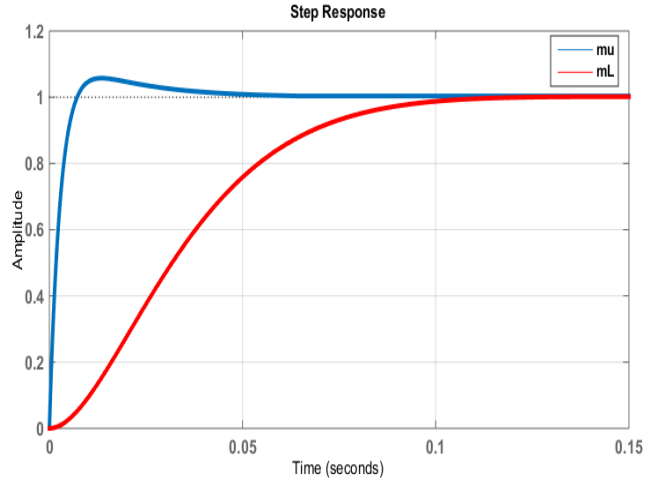

-a-

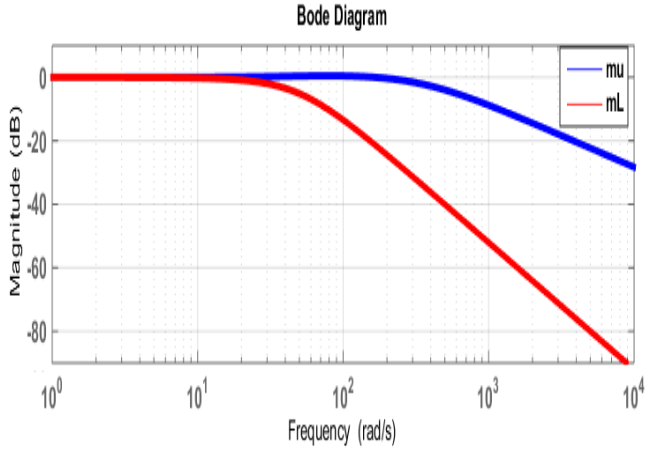

-b-

Fig. 7 –Reference tracking specification a) time domain, b) frequency domain

$$m_l(jw) \le \left| F(jw) \frac{P(j.w).G(j.w)}{1+P(j.w).G(j.w)} \right| \le m_u(jw) \qquad (11)$$
$$for \quad w > 0\, rd/s$$

The settling time requirements are bounded by the responses of the lower and upper models, which define the minimum and maximum acceptable times, respectively.

$$m_l(w) = \frac{384{,}6s + 19230{,}8}{s^2 + 398{,}7.s + 19230{,}8} \qquad (12)$$

$$m_u(w) = \frac{2500}{s^2 + 90.s + 2500} \qquad (13)$$

D. Controller design

The controller *G(s)* and prefilter were synthesized based on the most critical performance constraints. Figure (8) shows the resulting Nichols chart, which displays the design bounds and the compensated open-loop transfer function *P(s)G(s)* [6-16]:.

After the QFT bounds are determined, the nominal loop transfer function $P_0(s)$ is shaped by adding appropriate poles and zeros. This ensures a stable nominal closed-loop system that satisfies all performance bounds.

Subsequently, the robust tracking specifications are used to calculate magnitude bounds for the prefilter, *F(s)*. The synthesized prefilter must lie within the upper and lower bounds, $m_u(\omega)$ and $m_l(\omega)$. The resulting controller for the g(s) element incorporates a first-order high-pass filter [6-16]:.

$$g(s) = \frac{5.(\frac{s}{12}+1)}{s.(\frac{s}{973.875}+1).(\frac{s}{15725.7}+1)} \qquad (14)$$

And prefilter are :

$$f(s) = \frac{1}{\frac{s}{199}+1} \qquad (15)$$

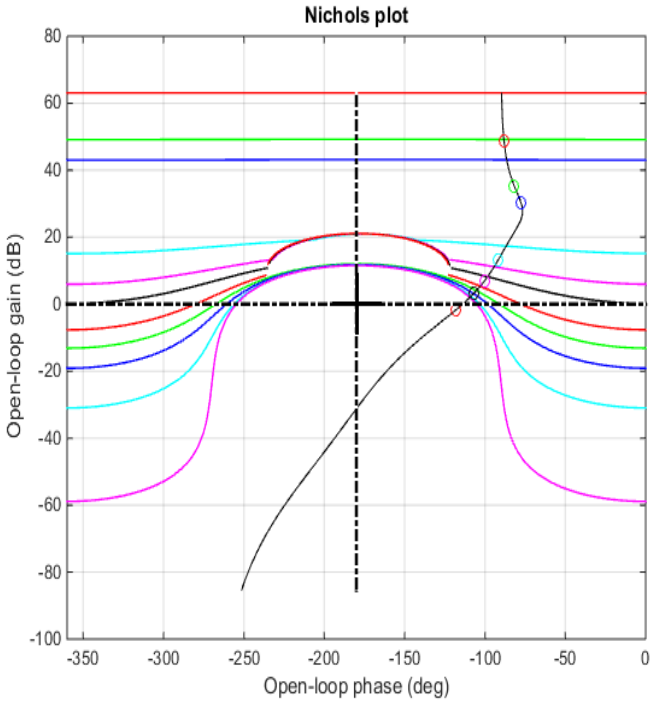

Fig. 8 – Loop-shaping design of SRM control

Figures (9) and (10) demonstrate how the control system, comprising *g(s)* and the QFT-designed prefilter *f (s)*, meets the performance specifications. Figure (9) presents the frequency-domain design, while Figure (10) validates the robust tracking performance through a time-domain analysis with some sample plants. The dashed blue curves are the same curves as in Figures (7.a) and (7.b).

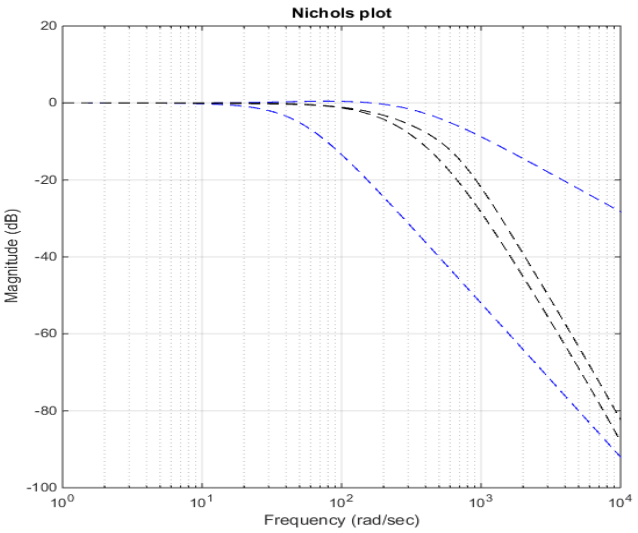

Fig. 9 – Pre-filter design of power control.

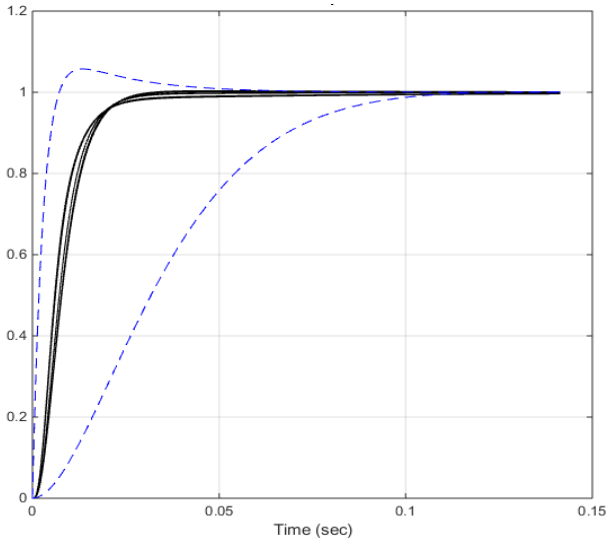

Fig. 10 –.Analysis of controller *g*(*s*) and prefilter *f*(*s*) for *p(s).* Reference tracking: m*u*, m*l*.

IV. Simulation Results

To evaluate the QFT controller's performance, the system depicted in Figure (1) was simulated. A no-load startup scenario was implemented using the MATLAB/Simulink environment.

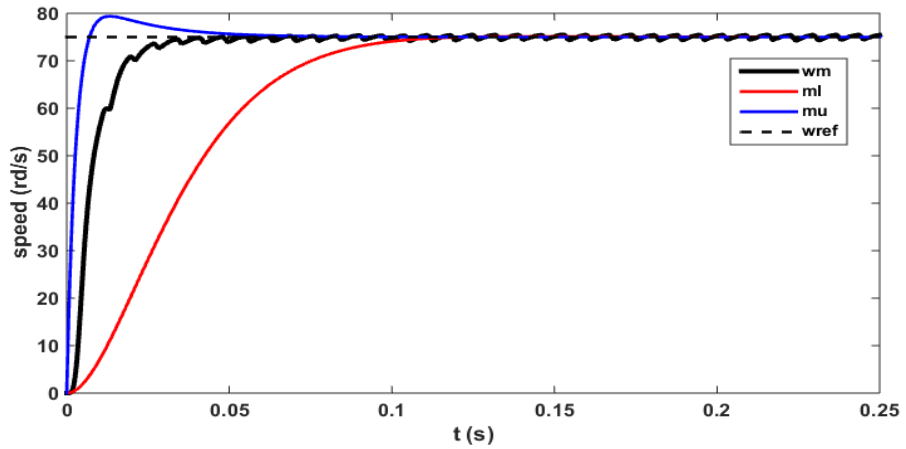

Fig. 11 Step Response of the system from 0 to 75 rd/s

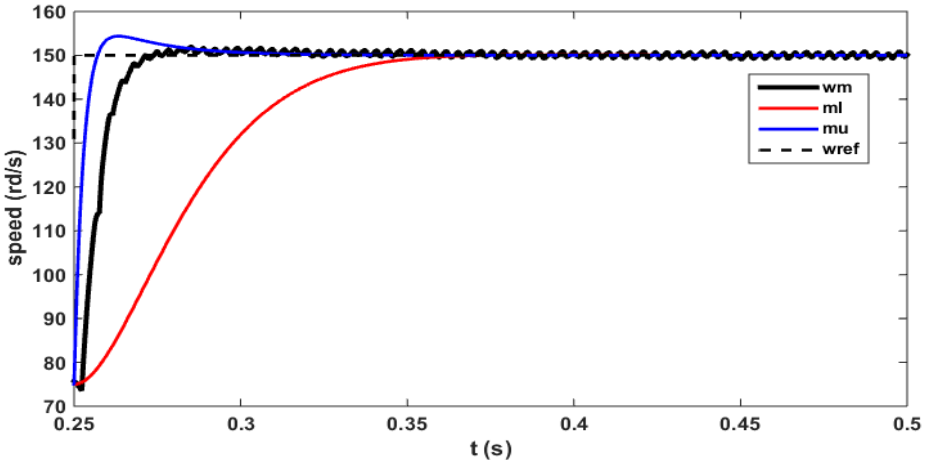

Fig. 12 Step Response of the system from 75 to 150 rd/s

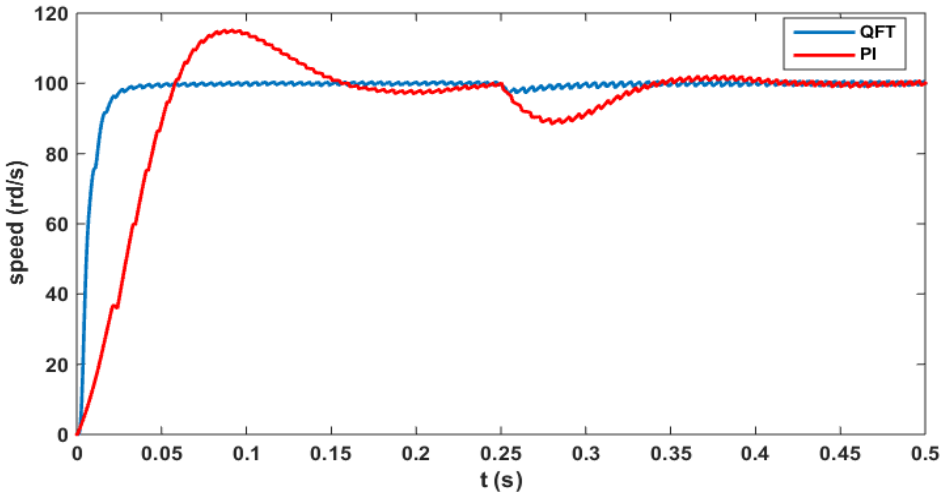

Fig. 13 Step Response of the system from 0 to 100 rd/s with load

Figure (11) and Figure (12), show the simulation step response of system, in all of the results, step responses are successfully placed between two tracking bounds.

Figure (13) shows the disturbance rejection capability of both QFT and PI (Kp=0,25 and Ki=3) controls operating at 100 rad/s and applying a sudden load torque of 1,5 N•m at 0,25 s.

Compared with conventional PI control, the response time of QFT control is faster than that of PI without overshoot, while PI has an overshoot of 12.5%.

And rhe QFT controller rapidly rejects the load disturbance with negligible steady-state error.

V. Conclusion

This paper introduces a novel robust speed control methodology for switched reluctance motors using Quantitative Feedback Theory. The proposed controller demonstrates a remarkable ability to simultaneously manage parametric uncertainties, external disturbances, and inherent system noise. Its architecture incorporates a digital implementation coupled with integral action, thus ensuring effective compensation of static errors. Simulation results highlight the robustness and tracking accuracy of the controller, surpassing those obtained with conventional approaches.

The Quantitative Feedback Theory (QFT) approach is distinguished by its inherent adaptability, enabling the maintenance of high dynamic performance despite variations in process parameters and load fluctuations. Furthermore, the QFT-based speed control strategy guarantees a fast, overshoot-free transient response while ensuring error elimination in steady state. These characteristics confirm the potential of QFT as a robust and efficient method for controlling nonlinear systems subject to uncertainties.

Appendix

Phase number 3; Number of stator poles 6; 30° pole arc; Number of rotor poles 4; 30° pole arc; Maximum inductance 8 mH (unsaturated); Minimum inductance 60 mH; Phase resistance $R = 1{,}3\ \Omega$; Moment of inertia J=0.0013Kg/m^2; Friction F=0,0183 Nm/s; Inverter voltage V=150V.

References

[1] A. Tahour, A.G. Aissaoui, Switched Reluctance Motor: Concept, Control and Applications, edition intechopen 2017, ISBN 978-953-51-3268-4, Print ISBN 978-953-51-3267-7, InTech Janeza Trdine 9, 51000 Rijeka, Croatia

[2] M. Garcia-Sanz and Constantine H. Houpis, Wind Energy Systems Control Engineering Design, CRC press, Taylor & Francis Group 2012.

[3] R. Krishnan, Switched reluctance motor drives modeling, simulation, analysis, design and applications. London: CRC Press; 2001.

[4] F. Soares and P.J. Costa Branco "Simulation of a 6/4 Switched Reluctance Motor Based on Matlab/Simulink Environment " aerospace and electronic system. IEEE transactions, Vol 37 pp989-1009, July 2001.

[5] Miller TJE. Switched reluctance motors and their control. Oxford: Oxford University Press; 1993.

[6] M. García-Sanz, Robust Control Engineering Practical QFT Solutions, Taylor & Francis Group 2017.

[7] C. H. Houpis and S. J. Rasmussen, Quantitative feedback theory, Fundamentals and Applications. New York: Marcel Dekker, 1999.

[8] O. Yaniv, Quantitative feedback design of linear and nonlinear control systems. Kluwer Academic, 1999.

[9] M V Chitra, Kapil Kumar Sharma, A Asok Kumar, Quantitative Feedback Theory Based Robust Control Design for a Flexible Launch Vehicle, 2015 International Conference on Control, Communication & Computing India (ICCC) | 19-21 November 2015.

[10] Gudimindla Hemachandra1, and Sharma K Manjunatha, Design and performance analysis of quantitative feedback theory based automated robust controller : An application to uncertain autonomous wind power system, AIMS Energy, Vol; 6, Issue 4, pp.:576-592. 2018, doi: 10.3934/energy.2018.4.576

[11] Ali Soltani Sharif ABADI, Pooyan Alinaghi HOSSEINABADI, Andrew ORDYS, Design a robust quantitative feedback theory controller for cyber-physical systems: ship course control problem, Archives of Control Sciences Volume 32(LXVIII), 2022 No. 3, pages *589–605*

[12] J. Elso, J. X. Ostolaza, Automatic synthesis of feedforward elements in quantitative feedback theory, International Journal of Robust and Nonlinear Control Volume 31, Issue 12, Aug 2021 Pages5523-6092

[13] C. Borghesani, Y. Chait, and O. Yaniv, The QFT frequency domain control design toolbox for use with MATLAB, user's guide. Terasoft, Inc 2003.

[14] C. Olalla, A. E. Aroudi, and R. Leyva, “QFT control for dc-dc buck converters,” in IEEE International Symposium on Circuits and Systems, ISCAS’06, 2006.

[15] C. Yeong-Hwa and C. Li-Wei, “QFT based robust controller design of series resonant dc/dc converters,” in Electric Machines and Drives Conference Record, 1997, IEEE International, 1997, pp. TC2/8.1–TC2/8.3.

[16] Caro Lucas, M. Modir Shanehchi, Peyman Asadi and Peyvand Mellati Rad, **A** Robust Speed Controller for Switched Reluctance Motor with Nonlinear QFT Design Approach, Thirty-Fifth IAS Annual Meeting and World Conference on Industrial Applications of Electrical Energy (Cat. No.00CH37129), Italy, 08-12 October 2000.